Article

# Enhanced Metal Ion Selectivity of 2,9-Di-(pyrid-2-yl)-1,10-phenanthroline and Its Use as a Fluorescent Sensor for Cadmium(II)

Gregory M. Cockrell, Gang Zhang, Donald G. VanDerveer, Randolph P. Thummel, and Robert D. Hancock

*J. Am. Chem. Soc.*, **2008**, 130 (4), 1420-1430 • DOI: 10.1021/ja077141m



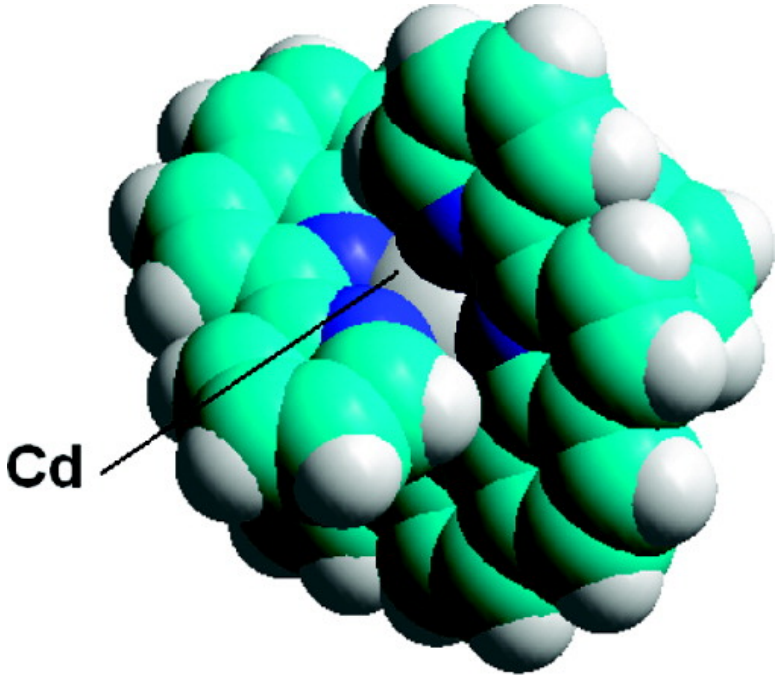

J|A|C|S
ARTICLES
Published on Web 01/05/2008

# Enhanced Metal Ion Selectivity of 2,9-Di-(pyrid-2-yl)-1,10-phenanthroline and Its Use as a Fluorescent Sensor for Cadmium(II)

Gregory M. Cockrell,[†] Gang Zhang,[‡] Donald G. VanDerveer,[§] Randolph P. Thummel,*[,‡] and Robert D. Hancock*[,†]

*Department of Chemistry and Biochemistry, University of North Carolina Wilmington, Wilmington, North Carolina, 28403, Department of Chemistry, University of Houston, Houston, Texas, and Department of Chemistry, Clemson University, Clemson, South Carolina 29634*

Received September 14, 2007; E-mail: hancockr@uncw.edu

***Abstract:*** The metal ion complexing properties of the ligand DPP (2,9-di-(pyrid-2-yl)-1,10-phenanthroline) were studied by crystallography, fluorimetry, and UV−visible spectroscopy. Because DPP forms five-membered chelate rings, it will favor complexation with metal ions of an ionic radius close to 1.0 Å. Metal ion complexation and accompanying selectivity of DPP is enhanced by the rigidity of the aromatic backbone of the ligand. $Cd^{2+}$, with an ionic radius of 0.96 Å, exhibits a strong CHEF (chelation enhanced fluorescence) effect with $10^{-8}$ M DPP, and $Cd^{2+}$ concentrations down to $10^{-9}$ M can be detected. Other metal ions that cause a significant CHEF effect with DPP are $Ca^{2+}$ ($10^{-3}$ M) and $Na^{+}$ (1.0 M), whereas metal ions such as $Zn^{2+}$, $Pb^{2+}$, and $Hg^{2+}$ cause no CHEF effect with DPP. The lack of a CHEF effect for $Zn^{2+}$ relates to the inability of this small ion to contact all four donor atoms of DPP. The structures of $[Cd(DPP)_2](ClO_4)_2$ (**1**), $[Pb(DPP)(ClO_4)_2H_2O]$ (**2**), and $[Hg(DPP)(ClO_4)_2]$ (**3**) are reported. The Cd(II) in **1** is 8-coordinate with the Cd−N bonds to the outer pyridyl groups stretched by steric clashes between the *o*-hydrogens on these outer pyridyl groups and the central aromatic ring of the second DPP ligand. The 8-coordinate Pb(II) in **2** has two short Pb−N bonds to the two central nitrogens of DPP, with longer bonds to the outer N-donors. The coordination sphere around the Pb(II) is completed by a coordinated water molecule, and two coordinated $ClO_4^-$ ions, with long Pb−O bonds to $ClO_4^-$ oxygens, typical of a sterically active lone pair on Pb(II). The Hg(II) in **3** shows an 8-coordinate structure with the Hg(II) forming short Hg−N bonds to the outer pyridyl groups of DPP, whereas the other Hg−N and Hg−O bonds are rather long. The structures are discussed in terms of the fit of large metal ions to DPP with minimal steric strain. The UV−visible studies of the equilibria involving DPP and metal ions gave formation constants that show that DPP has a higher affinity for metal ions with an ionic radius close to 1.0 Å, particularly Cd(II), Gd(III), and Bi(III), and low affinity for small metal ions such as Ni(II) and Zn(II). The complexes of several metal ions, such as Cd(II), Gd(III), and Pb(II), showed an equilibrium involving deprotonation of the complex at remarkably low pH values, which was attributed to deprotonation of coordinated water molecules according to: $[M(DPP)(H_2O)]^{n+} \leftrightarrows [M(DPP)(OH)]^{(n-1)+} + H^+$. The tendency to deprotonation of these DPP complexes at low pH is discussed in terms of the large hydrophobic surface of the coordinated DPP ligand destabilizing the hydration of coordinated water molecules and the build-up of charge on the metal ion in its DPP complex because of the inability of the coordinated DPP ligand to hydrogen bond with the solvent.

## Introduction

Sensing of metal ions by means of Chelation Enhanced Fluorescence (CHEF) is an active area of research,[1−18] which relates to the importance of metal ion sensing in biology, medicine, and the environment. Ligands bearing pyridyl groups and related substituents such as quinolyl groups, which have

[†] University of North Carolina Wilmington.
[‡] University of Houston.
[§] Clemson University.

(1) Thompson, R. B.; Bozym, R. A.; Cramer, M. L.; Stoddard, A. K.; Westerberg, N. M.; Fierke, C. A. *Fluoresc. Sens. Biosens*. **2006**, 107.
(2) Barrios, A. M. *ACS Chem. Biol*. **2006**, *1*, 67.
(3) Hilderbrand, S. A.; Lim, M. H.; Lippard, S. J. *Topics Fluoresc. Spectrosc*. **2005**, *9*, 163.
(4) Klonkowski, A. M.; Kledzik, K.; Gwiazda, M.; Orlowska, M. Annales Universitatis Mariae Curie-Sklodowska, Sectio AA: *Chemia* **2005**, *60*, 311.
(5) Meng, X.; Liu, L.; Guo, Q. *Huaxue Jinzhan* **2005**, *17*, 45.
(6) Prodi, L. *New J. Chem*. **2005**, *29*, 20.
(7) Parker, D.; Williams, J. A. G. *Metal Ions Biol. Syst*. **2003**, *40*, 233.
(8) Wang, Y.; Jin, W. *Huaxue Jinzhan* **2003**, *15*, 178.
(9) Kawakami, J.; Ito, S. *Curr. Topics Anal. Chem.* **2002**, *3*, 135.
(10) Rurack, K. *Spectrochim. Acta, Part A* **2001**, *57*, 2161.
(11) Burdette, S. C.; Lippard, S. J. *Coord. Chem. Rev.* **2001**, *216−217*, 333.
(12) Pina, F.; Bernardo, M. A.; Garcia-Espana, E. *Eur. J. Inorg. Chem.* **2000**, *10*, 2143.
(13) Roundhill, D. M. *Optoelectr. Prop. Inorg. Comp*. **1999**, 317.
(14) Purrello, R.; Gurrieri, S.; Lauceri, R. *Coord. Chem. Rev*. **1999**, *190−192*, 683.
(15) Fabbrizzi, L.; Licchelli, M.; Parodi, L.; Poggi, A.; Taglietti, A. *J. Fluoresc*. **1998**, *8*, 263.
(16) Alcock, N. W.; Clarke, A. J.; Errington, W.; Josceanu, A. M.; Moore, P.; Rawle, S. C.; Sheldon, P.; Smith, S. M.; Turonek, M. L. *Supramol. Chem*. **1996**, *6*, 281.
(17) Czarnik, A. W. *Trends Org. Chem.* **1993**, *4*, 123.
(18) Czarnik, A. W. *Adv. Supramol. Chem.* **1993**, *3*, 131.


**10.1021/ja077141m CCC: $40.75** 

the potential both of coordinating to the metal ion and of contributing to the CHEF effect, have been important in a variety of such applications.[19,20] In particular the sensing of $Cd^{2+}$ is of considerable interest because of its toxic nature.[5,21−32] The FAO/WHO Joint Expert Committee on Food Additives recommends[33] a maximum daily intake of Cd of 1.0−1.2 $\mu$g kg$^{-1}$ body mass. Current methods of analyzing for Cd mainly involve the use of AA (atomic absorption) or ICP (inductively coupled plasma) atomic emission spectroscopy, meaning that analysis must wait for results from a laboratory. Fluorescence is a convenient and accurate method of analysis for metal ions that takes advantage of the CHEF effect, and the instrumentation presents considerable potential for miniaturization for use in the field. The thrust of the present work is aimed primarily at the design of new ligands that display enhanced levels of selectivity and very strong binding of $Cd^{2+}$. These features might lead to the use of fluorescence to detect very low levels of $Cd^{2+}$.

The approach followed in ligand design is based on increased ligand preorganization,[34] derived from the rigid ligand backbone present in polyazaaromatic ligands such as 1,10-phenanthroline. The recently reported[35] metal ion complexing properties of PDA (see Figure 1 for ligand abbreviations) show that complexes of greatly enhanced thermodynamic stability result because of the rigidity of the ligand backbone. An important aspect of PDA is that a macrocyclic structure is not necessary for achieving high levels of preorganization and for enhanced selectivity in binding metal ions of the appropriate size. The size selectivity of PDA is based on the fact that it forms three rigid five-membered chelate rings, which favor[35−37] larger metal ions with an ionic radius[38] ($r^+$) of about 1.0 Å. It has been noted[36,37] that five-membered chelate rings favor the complexation of larger metal ions whereas six-membered chelate rings favor the complexation of smaller metal ions. This is summarized[35] for chelate rings of the type discussed here in terms of the graphic below:

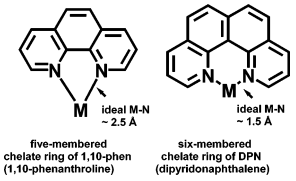


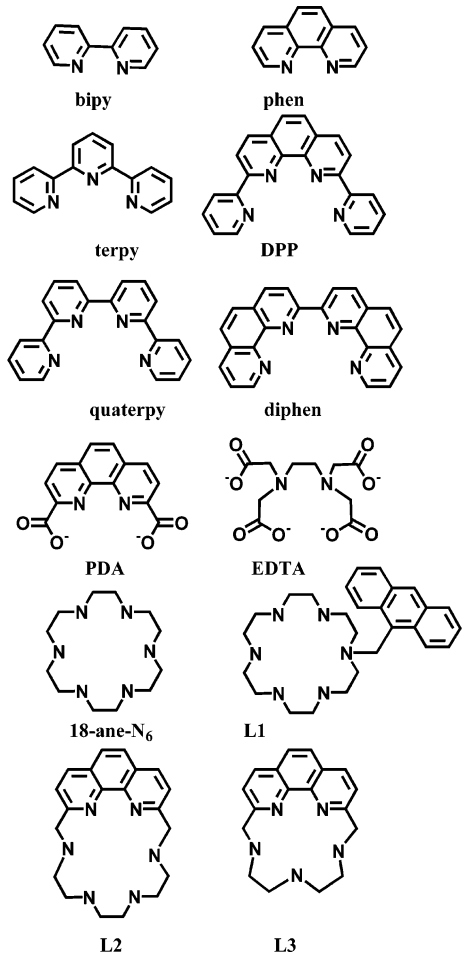


***Figure 1.*** Ligands discussed in this paper.

The ligand DPP (Figure 1) has been reported[39] as part of a study on Ru(II) complexes. DPP, like PDA, is based on phen, and the five-membered rings should promote selectivity for the large $Cd^{2+}$ ion ($r^+ = 0.96$ Å) over $Zn^{2+}$ ($r^+ = 0.74$ Å). This selectivity is important, because most ligands show little difference in log $K_1$ (the formation constant[40]) between $Zn^{2+}$ and $Cd^{2+}$. Thus, an N-donor macrocyclic ligand bearing an anthracenyl group as a fluorophore[41] (L1 in Figure 1) showed little selectivity between $Zn^{2+}$ and $Cd^{2+}$ at neutral pH values. This result is not unexpected because 18-ane-$N_6$, the parent macrocycle of L1 without an anthracenyl group, gives log $K_1$ for $Zn^{2+}$ and $Cd^{2+}$ of 18.7 and 18.8, respectively.[40] In using L1 to detect $Cd^{2+}$, interference from $Zn^{2+}$ could be eliminated[41] only by raising the pH of the sample to 13, where Zn may be removed from L1 by the formation of a zincate anion. PDA is a remarkable tetradentate ligand that complexes many metal ions

(19) Nolan, E. M.; Jaworski, J.; Racine, M. E.; Sheng, M.; Lippard, S. J. *Inorg. Chem.* **2006**, *45*, 9748.
(20) Gan, W.; Jones, S. B.; Reibenspies, J. H.; Hancock, R. D. *Inorg. Chim. Acta* **2005**, *358*, 3958.
(21) Garcia-Reyes, J. F.; Ortega-Barrales, P.; Molina-Diaz, A. *Microchem. J.* **2006**, *82*, 94.
(22) Costero, A. M.; Banuls, M. J.; Aurell, M. J.; Ochando, L. E.; Domenech, A. *Tetrahedron* **2005**, *61*, 10309.
(23) Kubo, Y.; Ishida, T.; Kobayashi, A.; James, T. D. *J. Mater. Chem.* **2005**, *15*, 2889.
(24) Bronson, R. T.; Michaelis, D. J.; Lamb, R. D.; Husseini, G. A.; Farnsworth, P. B.; Linford, M. R.; Izatt, R. M.; Bradshaw, J. S.; Savage, P. B. *Org. Lett.* **2005**, *7*, 1105.
(25) Van Arman, S. A.; Sisk, T. M.; Zawrotny, D. M. *Lett. Org. Chem.* **2005**, *2*, 54.
(26) Gunnlaugsson, T.; Lee, T. C.; Parkesh, R. *Tetrahedron* **2004**, *60*, 11239.
(27) Costero, A. M.; Sanchis, J.; Gil, S.; Sanz, V.; Ramirez de Arellano, M. C.; Williams, J. A. G. *Supramol. Chem.* **2004**, *16*, 435.
(28) Aoki, S.; Kagata, D.; Shiro, M.; Takeda, K.; Kimura, E. *J. Am. Chem. Soc.* **2004**, *126*, 13377.
(29) Costero, A. M.; Gil, S.; Sanchis, J.; Peransi, S.; Sanz, V.; Williams, J. A. G. *Tetrahedron* **2004**, *60*, 6327.
(30) Mizukami, S.; Nagano, T.; Urano, Y.; Odani, A.; Kikuchi, K. *J. Am. Chem. Soc.* **2002**, *124*, 3920.
(31) Wang, Y.; Astilean, S.; Haran, G.; Warshawsky, A. *Anal. Chem.* **2001**, *73*, 4096.
(32) Zhujun, Z.; Seitz, W. R. *Anal. Chim. Acta* **1985**, *171*, 251.
(33) *Guidelines for drinking water quality*, 2nd ed.; Health Criteria and Other Supporting Information, Vol. 2; World Health Organization: Geneva, 1998; p 281.
(34) Cram, D. J.; Cram, J. M. *Acc. Chem. Res.* **1978**, *11*, 49.
(35) Melton, D. L.; VanDerveer, D. G.; Hancock, R. D. *Inorg. Chem.* **2006**, *45*, 9306.
(36) Hancock, R. D. *Acc. Chem. Res.* **1990**, *26*, 875.
(37) Hancock, R. D.; Martell, A. E. *Chem. Rev.* **1989**, *89* 1875.
(38) Shannon, R. D. *Acta Crystallogr., Sect. A* **1976**, *32*, 751.
(39) Zong, R.; Thummel, R. P. *J. Am. Chem. Soc.* **2004**, *126*, 10800.
(40) Martell, A. E.; Smith, R. M. *Critical Stability Constant Database, 46*; National Institute of Science and Technology (NIST): Gaithersburg, MD, 2003.
(41) Charles, S.; Yunus, S.; Dubois, F.; Vander Donckt, E. *Anal. Chim. Acta* **2001**, *440*, 37.

***Table 1.*** Crystal Data and Details of Structure Refinement for $[Cd(DPP)_2](ClO_4)_2$ (**1**), $[Pb(DPP)(H_2O)](ClO_4)_2$ (**2**), and $[Hg(DPP)(ClO_4)_2]$ (**3**)

| | 1 | 2 | 3 |
|---|---|---|---|
| empirical formula | $C_{44}H_{28}N_8CdCl_2O_8$ | $C_{22}H_{16}PbCl_2N_4O_9$ | $C_{22}H_{14}HgCl_2N_4O_8$ |
| formula weight | 980.04 | 758.49 | 733.86 |
| temperature (K) | 163(2) | 158(2) | 153(2) |
| wavelength (Å) | 0.7107 | 0.71073 | 0.71073 |
| crystal system | orthorhombic | monoclinic | monoclinic |
| space group | *Ccca* | $P2_1/c$ | $P2_1/c$ |
| unit cell dimensions | | | |
| *a* (Å) | 16.617(3) | 15.715(3) | 13.651(3) |
| *b* (Å) | 19.661(4) | 11.425(2) | 11.338(2) |
| *c* (Å) | 12.120(2) | 27.309(6) | 15.033(3) |
| $\beta$ (deg) | 90 | 104.72(3) | 107.58(3) |
| volume (Å$^3$) | 3959.7(14) | 4742.0(16) | 2218.1(8) |
| *Z* | 4 | 8 | 4 |
| final *R* indices [$I > 2\sigma(I)$] | $R1 = 0.0367$ | $R1 = 0.0597$ | $R1 = 0.0803$ |
| | $wR2 = 0.0734$ | $wR2 = 0.1016$ | $wR2 = 0.1791$ |
| *R* indices (all data) | $R1 = 0.0321$ | $R1 = 0.0515$ | $R1 = 0.0652$ |
| | $wR2 = 0.0705$ | $wR2 = 0.0985$ | $wR2 = 0.1622$ |

at neutral pH as strongly as does the hexadentate EDTA. The combination of "hard"[42] acetate groups and fairly "soft" pyridyl N-donors on PDA parallels the donor mix on EDTA, giving it a high affinity in aqueous solution for virtually all metal ions, whether soft or hard.

The presence of only fairly soft pyridyl groups on DPP should shift affinity away from hard metal ions and thus enhance the metal binding affinity for the soft $Cd^{2+}$ ion as compared to other metal ions such as $Ca^{2+}$ or $Mg^{2+}$ present in natural waters or biological systems. Complexation of $Cd^{2+}$ over the omnipresent $Zn^{2+}$ should be favored by the size-based selectivity of DPP toward larger metal ions based on chelate ring size.[35−37] Of considerable interest is the extent to which the greater preorganization present in DPP will increase thermodynamic complex stability and metal ion selectivity as compared to less preorganized analogs such as quaterpy or terpy. DPP does not have a cavity as do macrocycles but rather can be regarded as having a highly preorganized cleft with a potential preference for metal ions of a definite size. In this paper, we report a study of DPP selectively sensing $Cd^{2+}$ by the CHEF effect, the thermodynamics of complexation of metal ions by DPP in aqueous solution, and the structures of the DPP complexes of Cd(II), Pb(II), and Hg(II).

## Experimental Section

**Materials.** The synthesis of DPP has been described elsewhere.[39] The metal perchlorates were obtained from VWR or Strem in ≥99% purity and used as received. All solutions were made up in deionized water (Milli-Q, Waters Corp.) of >18 MΩ.cm$^{-1}$ resistivity.

**Synthesis of Complexes of DPP.** The general procedure followed for the synthesis of Cd(II), Pb(II), and Hg(II) complexes with DPP was as follows. One equivalent of DPP (about 10 mg) was dissolved in *n*-butanol (20 mL), and one equivalent of the metal perchlorate was dissolved in deionized water (20 mL). The aqueous solution of the metal perchlorate was placed in a 50 mL beaker, and the *n*-butanol solution of DPP was carefully layered on top of the water layer. The beaker was covered with Parafilm and then left to stand. After a few days, crystals of the DPP complex formed at the interface of the solvents, and some crystals began to fall to the bottom of the beaker. The solutions were filtered under vacuum and air-dried.

**$[Cd(DPP)_2](ClO_4)_2$ (1).** Colorless crystals. Elemental analysis, calcd for $C_{44}H_{28}CdCl_2N_8O_8$: C, 53.92; H, 2.88; N 11.43%. Found: C, 54.11; H, 2.91; N, 11.29%.

***Table 2.*** Selected Bond Lengths (Å) and Angles (deg)[a] in $[Cd(DPP)_2](ClO_4)_2$ (**1**)

| | | | |
|---|---|---|---|
| Cd(1)−N(2) | 2.412(2) | Cd(1)−N(1) | 2.559(2) |
| N(2)−Cd(1)−N(1) | 64.93(7) | N(2)−Cd(1)−N(2) | 68.22(10) |
| N(1)−Cd(1)−N(1) | 162.88(10) | N(2)−Cd(1)−N(1)# | 88.70(7) |
| N(1)−Cd(1)−N(1)# | 92.21(11) | N(2)−Cd(1)−N(2)# | 125.34(10) |

[a] A "#" indicates atom is from the second DPP coordinated to the same Cd atom.

**$[Pb(DPP)(H_2O)](ClO_4)_2$ (2).** Colorless crystals. Elemental analysis, calcd for $C_{22}H_{16}PbCl_2N_8O_9$: C, 34.84; H, 2.13; N 7.39%. Found: C, 34.73; H, 2.46; N, 7.35%.

**$[Hg(DPP)](ClO_4)_2$ (3).** Colorless crystals. Elemental analysis, calcd for $C_{22}H_{14}HgCl_2N_8O_8$: C, 36.01; H, 1.92; N 7.63%. Found: C, 36.05; H, 1.94; N, 7.77%.

**Molecular Structure Determination.** A Rigaku Mercury diffractometer, using the omega scan mode, was employed for crystal screening, unit cell determination, and data collection. The structure was solved by direct methods and refined to convergence.[43] Some details of the structure determination are given in Table 1, and crystal coordinates and details of the structure determination of **1**−**3** have been deposited with the CSD (Cambridge Structural Database).[44] A selection of bond lengths and angles for **1**, **2**, and **3** are given in Tables 2−4. The structures of **1**−**3** are shown in Figures 2−4.

**Fluorescence Measurements.** Excitation−emission matrix (EEM) fluorescence properties were determined on a Jobin Yvon SPEX Fluoromax-3 scanning fluorometer equipped with a 150 W Xe arc lamp and a R928P detector. The instrument was configured to collect the signal in ratio mode with dark offset using 5 nm bandpasses on both the excitation and emission monochromators. The EEMs were created by concatenating emission spectra measured every 5 nm from 250 to 500 nm at 51 separate excitation wavelengths. Scans were corrected for instrument configuration using factory supplied correction factors. Postprocessing of scans was performed using the FLToolbox program.[45] The software eliminates Rayleigh and Raman scattering peaks by excising portions (±10−15 nm FW) of each scan centered on the respective scatter peak. The excised data is replaced using three-dimensional interpolation of the remaining data according to the Delaunay triangulation method and constraining the interpolation such that all nonexcised data is retained. Following removal of scatter peaks, data were normalized to a daily determined water Raman intensity (275ex/303em, 5 nm bandpasses) and converted to Raman normalized

(42) Pearson, R. G. *Chemical Hardness*; Wiley-VCH: Weinheim, 1997.
(43) Gabe, E. J.; Le Page, Y.; Charland, J.-P.; Lee, F. L.; White, P. S. *J. Appl. Crystallogr.* 1989, **22**, 384.
(44) Cambridge Crystallographic Data Centre, 12 Union Road, Cambridge CB2 1EZ, United Kingdom.
(45) Sheldon, W. *MATLAB*, release 11; University of Georgia: Athens, GA, 1999.

***Table 3.*** Selected Bond Lengths (Å) and Angles (deg) in $[Pb(DPP)(H_2O)(ClO_4)_2]$ (**2**)

| | | | | | |
|---|---|---|---|---|---|
| Pb(1)−N(1) | 2.661(7) | Pb(1)−N(2) | 2.522(7) | Pb(1)−N(3) | 2.487(7) |
| Pb(1)−N(4) | 2.621(8) | Pb(1)−O(1) | 2.382(7) | Pb(2)−O(2) | 2.477(6) |
| Pb(2)−N(5) | 2.644(8) | Pb(2)−N(6) | 2.560(7) | Pb(2)−N(7) | 2.533(8) |
| Pb(2)−N(8) | 2.657(8) | Pb(2)−O(3) | 2.642(7) | | |
| N(2)−Pb(1)−N(1) | 62.5(2) | N(3)−Pb(1)−N(2) | 65.7(2) | | |
| N(3)−Pb(1)−N(4) | 63.4(3) | O(1)−Pb(1)−N(3) | 86.3(2) | | |
| O(1)−Pb(1)−N(2) | 83.9(2) | O(1)−Pb(1)−N(4) | 74.3(2) | | |
| N(6)−Pb(2)−N(5) | 62.0(2) | N(7)−Pb(2)−N(6) | 66.1(2) | | |
| N(7)−Pb(2)−N(8) | 63.1(3) | O(2)−Pb(2)−N(7) | 81.0(2) | | |
| O(2)−Pb(2)−N(6) | 75.5(2) | O(2)−Pb(2)−N(5) | 82.6(3) | | |
| N(7)−Pb(2)−O(3) | 78.1(3) | N(6)−Pb(2)−O(3) | 73.7(2) | | |

***Table 4.*** Selected Bond Lengths (Å) and Angles (deg) in $[Hg(DPP)(ClO_4)_2]$ (**3**)

| | | | | | |
|---|---|---|---|---|---|
| Hg(1)−N(1) | 2.249(10) | Hg(1)−N(4) | 2.258(10) | Hg(1)−N(3) | 2.397(9) |
| Hg(1)−N(2) | 2.425(11) | Hg(1)−O(7) | 2.653(8) | | |
| N(1)−Hg(1)−N(4) | 155.2(4) | N(1)−Hg(1)−N(3) | 135.3(4) | | |
| N(4)−Hg(1)−N(3) | 68.9(3) | N(1)−Hg(1)−N(2) | 68.9(4) | | |
| N(4)−Hg(1)−N(2) | 135.7(4) | N(3)−Hg(1)−N(2) | 66.8(4) | | |
| N(1)−Hg(1)−O(7) | 97.5(3) | N(4)−Hg(1)−O(7) | 90.4(3) | | |
| N(3)−Hg(1)−O(7) | 82.5(3) | N(2)−Hg(1)−O(7) | 82.9(3) | | |

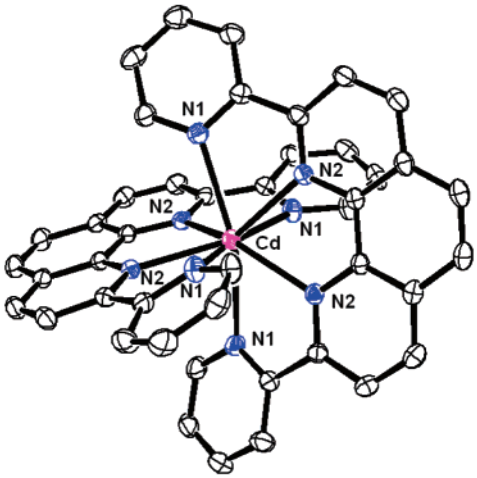


***Figure 2.*** ORTEP[48] drawing of the complex cation $[Cd(DPP)_2]^{2+}$ from **1**, showing the numbering of the donor atoms around Cd. H-atoms omitted for clarity. Thermal ellipsoids are drawn at 50% probability level.

quinine sulfate equivalents (QSE) in ppb. Replicate scans were generally within 5% agreement in terms of intensity and within bandpass resolution in terms of peak location.

**Formation Constant Determination.** These were determined by UV−visible spectroscopy following procedures similar to those of Choppin et al.[46] for studying phen complexes. UV-visible spectra were recorded using a Varian 300 Cary 1E UV-Visible Spectrophotometer controlled by Cary Win UV Scan Application version 02.00(5) software. A VWR sympHony SR60IC pH meter with a VWR sympHony gel epoxy semi-micro combination pH electrode was used for all pH readings, which were made in the external titration cell, with $N_2$ bubbled through the cell to exclude $CO_2$. The pH meter was calibrated prior to every titration using standard acid−base titration methods. The titration cell containing 50 mL of ligand/metal solution was placed in a bath thermostatted to 25.0 ± 0.1 °C, and a peristaltic pump was used to circulate the solution through a 1 cm quartz flow cell situated in the spectrophotometer. The pH was altered in the range 2−10 by additions to the external titration cell of small amounts of $HClO_4$ or NaOH as required using a micropipette. After each adjustment of pH, the system was allowed to mix by operation of the peristaltic pump for 15 min prior to recording the spectrum, and the cell was also agitated with a magnetic stirrer bar to ensure complete mixing.

(46) Xia, Y. X.; Chen, J. F.; Choppin, G. R. *Talanta* **1996**, *43*, 2073.

DPP is not very water soluble (~$10^{-5}$ M), but has intense bands in the UV that can be used to monitor complex formation in solution. The variation of the spectra of $4 \times 10^{-6}$ M DPP solutions as a function of pH in 0.1 M $NaClO_4$ at 25 °C is seen in Figure 5a. Two protonation constants of DPP were determined from the variation in absorbance as a function of pH at five different wavelengths (Table 5). Fitting of theoretical absorbance versus pH curves was accomplished using the SOLVER module of EXCEL.[47] For a set of spectra for any one metal ion with PDA, SOLVER was used to fit protonation constants and molar absorbtivities for the species in solution involving DPP. The standard deviations given for log K values in Table 5 were calculated using the SOLVSTAT macro provided with ref 47.

The two protonation constants for DPP, $K_{a1}$ and $K_{a2}$, were obtained by fitting them plus the molar absorbtivities (MA(L), MA(LH), and $MA(LH_2)$) of the species L, LH, and $LH_2$ (L = DPP) in eq 2 to a set of curves of absorbance (Abs) as a function of pH.

$$\text{Abs} = [\text{L}].\text{MA(L)} + [\text{LH}].\text{MA(LH)} + [\text{LH}_2].\text{MA(LH}_2) \quad (1)$$

$$= [\text{L}].\text{MA(L)} + K_{a1}\,[\text{L}][\text{H}^+].\text{MA(LH)} + K_{a1}.K_{a2}.[\text{L}][\text{H}^+].^2\text{MA(LH}_2) \quad (2)$$

In the presence of metal ions, the two apparent protonation constants are still present but shifted to lower pH by competition with the metal ion. In addition, for some metal ions, an additional protonation equilibrium at higher pH was observed, which was attributed to deprotonation of waters coordinated to the metal ion according to eq 3.

$$\text{ML}^{n+} = \text{ML(OH)}^{(n-1)+} + \text{H}^+ \quad (3)$$

These pH-dependent equilibria with the metal ions present were once again fitted using SOLVER.[47] As described previously,[35] it is then a simple matter to calculate log $K_1$ for the metal ions from the equilibria corresponding to eq 4 and the measured values of p$K_1$ and p$K_2$ for DPP.

$$\text{ML} + 2\,\text{H}^+ = \text{M} + \text{LH}_2^{2+} \quad (4)$$

Determination of log $K_1$ for the Cd(II)/DPP complex was challenging because this persisted with only a small amount of dissociation even at pH 1.0. Competition experiments with EDTA, as were used[35] to

(47) Billo, E. J. *EXCEL for Chemists*; Wiley-VCH: New York, 2001.
(48) *ORTEP-3 for Windows*, version 1.08; Farrugia, L. J. *J. Appl. Cryst.* **1997**, *30*, 565.

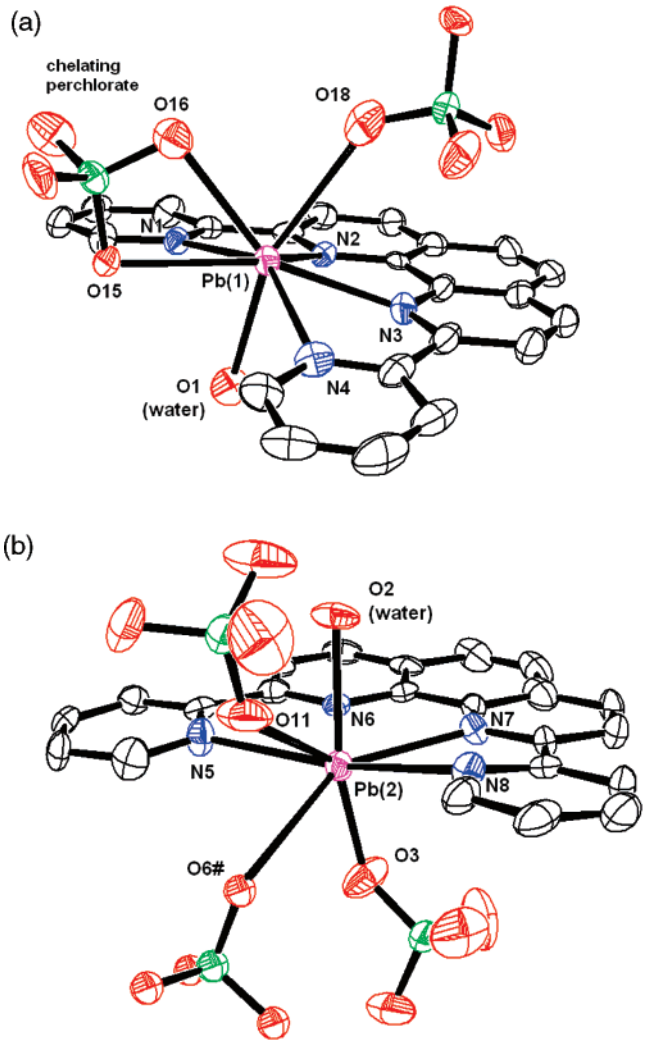


***Figure 3.*** (a) ORTEP[48] drawing of the complex $[Pb(1)(DPP)(H_2O)(ClO_4)_2]$ in **2**, showing the numbering of the donor atoms around Pb(1). O(1) is from a coordinated water molecule. H-atoms are omitted for clarity. Thermal ellipsoids are drawn at 50% probability. (b) ORTEP[48] drawing of the complex $[Pb(2)(DPP)(H_2O)(ClO_4)_2]$ in **2**, showing the numbering of the donor atoms around Pb(2). O(2) is from a coordinated water molecule. H-atoms are omitted for clarity. A bridging perchlorate from an adjacent $[Pb(2)(DPP)(H_2O)(ClO_4)_2]$ individual was included to complete the coordination sphere (O6#). The lone pair on Pb(2) is thought to lie between the long bonds from Pb(2) to O(3), O(11), and O(6)#, as discussed in the text. Thermal ellipsoids are drawn at 50% probability.

measure log $K_1$ for complexes of PDA, proved fruitless, because the Cd(II) DPP complex was unaffected by even a $10^4$ excess of EDTA. It was found that the Cd(II)/DPP complex dissociated into $Cd^{2+}$ and $LH_2^{2+}$ in concentrations of $HClO_4$ in excess of 1 M. These were used to confirm that the Cd(II)/DPP complex had indeed dissociated to a small extent at pH 1.0, and this extent of dissociation was used to calculate the value of log $K_1$ for the Cd(II)/DPP complex in Table 5. The Bi(III)/DPP complex was unaffected even by 1.0 M $HClO_4$, and thus, a different strategy was used to determine log $K_1$ for the Bi(III) complex. A solution containing $4 \times 10^{-6}$ M of each of DPP and Bi(III) was titrated with 0.0333 M $Cd^{2+}$, and the UV visible spectra followed as the spectrum changed from that of the Bi(III) complex with no $Cd^{2+}$ added to that of the Cd(II)/DPP complex in a large excess of $Cd^{2+}$. From the variation of absorbance at five different wavelengths, log $K$ for eq 5 was calculated to be $-2.6 \pm 0.2$, which gave the very high value of log $K_1 = 14.6$ for the Bi(III)/DPP complex in Table 5.

$$Bi(DPP)^{3+} + Cd^{2+} = Bi^{3+} + Cd(DPP)^{2+} \quad (5)$$

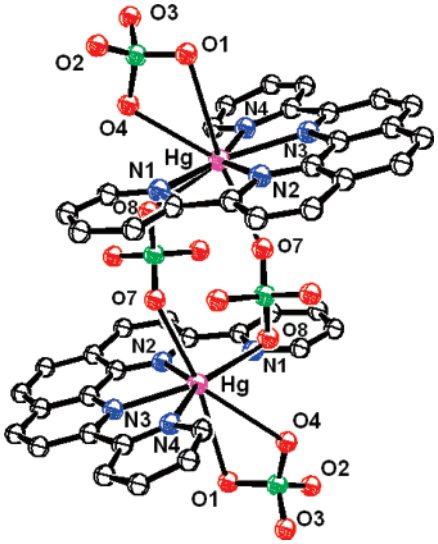


***Figure 4.*** ORTEP[48] drawing of the complex $[Hg(DPP)(ClO_4)_2]$ (**3**), showing the numbering of the donor atoms around Hg. H-atoms are omitted for clarity. Two $[Hg(DPP)(ClO_4)_2]$ individuals are shown to illustrate the bridging of the perchlorate groups. Thermal ellipsoids not shown.

## Results and Discussion

**Formation Constants.** The electronic spectra of DPP and its metal ion complexes showed distinctive features, confirming the presence of a coordinated metal ion, even for weak complexes as in the case of $Ca^{2+}$. Figure 5a shows the spectra of $6 \times 10^{-4}$ M DPP in 0.1 M $NaClO_4$ as a function of pH. The strong band at 277 nm is attributed to in the diprotonated ligand. In Figure 6a, the Gd(III) complex shows the remarkable spectral changes accompanying complex formation. The bands present in the diprotonated DPP ligand are replaced by similar bands on complex formation, which occur at about the same wavelength but are much sharper than those of the diprotonated ligand. This behavior is typical for metal ions that are of about the right size to coordinate in a low-strain manner in the cleft of DPP, namely those with an ionic radius ($r^+$) of not much less than 1.0 Å. This type of behavior is observed for all the metal ions studied, whose log $K$ values with DPP are reported in Table 5, except for the small[38] metal ions $Ni^{2+}$ ($r^+ = 0.67$ Å) and $Zn^{2+}$ ($r^+ = 0.74$ Å). This observation suggests that the band sharpening seen in Figure 6a reflects a stiffening of the DPP ligand by coordination to the metal ion, which in turn affects the vibrations that normally are responsible for the broadening of electronic transitions to which the vibrations are coupled. Although not commented on previously,[35] a similar but much less marked band sharpening is observed for PDA on formation of complexes with metal ions. For a small metal ion such as $Zn^{2+}$ (Figure 7), the electronic spectrum does not show peak sharpening as the complex forms, in accord with the idea that the metal ion cannot make strong contact with all four donor atoms of DPP simultaneously.

All of the sets of spectra, as in Figure 6a for Gd(III)/DPP, transition from the spectrum of the DPP complex to that of the diprotonated free ligand as the pH is lowered. It was from these equilibria, corresponding to eq 4 in the experimental section, that the formation constants in Table 5 were calculated. What was quite unexpected was that the DPP complexes of several metal ions, namely Cd(II), Gd(III), Lu(III), Pb(II), and In(III), showed an additional deprotonation equilibrium at a surprisingly

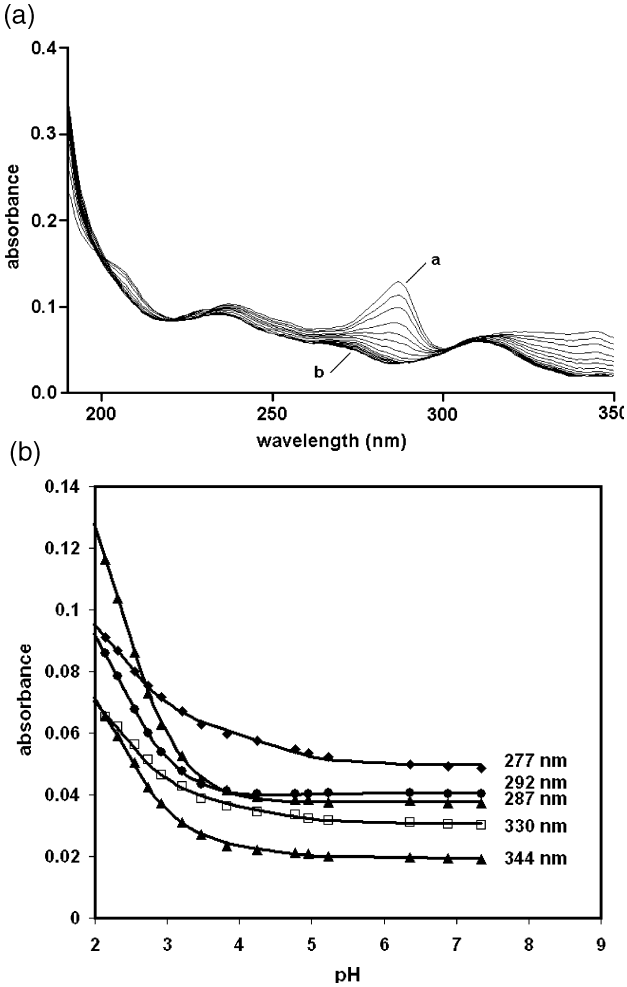


***Figure 5.*** (a) Electronic spectra of solutions of $4.0 \times 10^{-6}$ M DPP in 0.1 M $NaClO_4$ in the pH range 1.99 (spectrum "a") to 7.34 (spectrum "b"). (b) Variation of absorbance of $4 \times 10^{-6}$ M DPP (= L) solution as a function of pH at five different wavelengths. The solid lines are theoretical curves fitted using SOLVER[47] with protonation constants of 4.58 and 2.35, plus molar absorbtivities for the L, $LH^+$, and $LH_2^{2+}$ species at each wavelength. A value of $R^2$ of 0.9995 for the fit was obtained.

low pH (eq 3). The inflections at pH 5.17 for the Gd(III)/DPP complex in Figure 6b show this equilibrium. This equilibrium seemed unlikely to involve the ligand, because these protonation equilibria generally occurred well above the first protonation constant of the ligand, so would therefore not involve the formation of $MLH^+$ monoprotonated DPP complexes. The most reasonable suggestion is that these equilibria involve deprotonation of waters coordinated to the metal ion. What is remarkable is the low pH at which these deprotonations are occurring. In fact, they occur at much lower pH values than are found for any other complexes with the same metal ions, or for the aquo ions themselves.[40] Table 6 compares the $pK_a$ values of the metal aqua ions with the $pK_a$ values of the DPP complexes. The large hydrophobic surface of the coordinated DPP ligand may disrupt the hydration of adjacent waters coordinated to the metal ions in the DPP complexes. This disruption could destabilize the complex $[M(DPP)(OH_2)_x]^{n+}$ with its higher positive charge, and thus promote loss of a proton to give the lower charged hydroxy species $[M(DPP)(OH_2)_{(x-1)}(OH)]^{(n-1)+}$. A further factor may be that coordinated DPP is incapable of H-bonding to the solvent. This H-bonding is an important factor in stabilizing the charged metal aqua ions,[37] and its absence may lead to higher positive

***Table 5.*** Protonation and Formation Constants Determined Here for DPP[a] (L)

| equilibrium | | | log *K* | reference |
|---|---|---|---|---|
| $H^+ + OH^-$ | = | $H_2O$ | 13.78 | 40 |
| $L + H^+$ | = | $LH^+$ | 4.58(7) | this work |
| $LH^+ + H^+$ | = | $LH_2^{2+}$ | 2.35(2) | this work |
| $Ca^{2+} + L$ | = | $CaL^{2+}$ | 2.9(1) | this work |
| $La^{3+} + L$ | = | $LaL^{3+}$ | 5.1(1) | this work |
| $LaLOH^{3+} + H^+$ | = | $LaL^{3+}$ | >6 | this work |
| $Gd^{3+} + L$ | = | $GdL^{3+}$ | 6.2(1) | this work |
| $GdLOH^{2+} + H^+$ | = | $GdL^{3+}$ | 5.1(5) | this work |
| $Lu^{3+} + L$ | = | $LuL^{3+}$ | 5.3(1) | this work |
| $LuLOH^{2+} + H^+$ | = | $LuL^{3+}$ | 5.5(1) | this work |
| $Mn^{2+} + L$ | = | $MnL^{2+}$ | 6.4(1) | this work |
| $Ni^{2+} + L$ | = | $NiL^{2+}$ | 6.8(1) | this work |
| $Zn^{2+} + L$ | = | $ZnL^{2+}$ | 8.7(1) | this work |
| $Cd^{2+} + L$ | = | $CdL^{2+}$ | 12.2(1) | this work |
| $CdLOH^+ + H^+$ | | $CdL^{2+}$ | 6.0(1) | this work |
| $Pb^{2+} + L$ | = | $PbL^{2+}$ | 7.8(1) | this work |
| $PbLOH^+ + H^+$ | = | $PbL^{2+}$ | 5.70(4) | this work |
| $In^{3+} + L$ | = | $InL^{3+}$ | 8.3(1) | this work |
| $InLOH^{2+} + H^+$ | = | $InL^{3+}$ | 3.24(3) | this work |
| $Bi^{3+} + L$ | = | $BiL^{3+}$ | (14.8(3)) | this work |

[a] In 0.1 M $NaClO_4$ at 25.0 °C. DPP = 2,9-bis(2-pyridinyl)-1,10-phenanthroline.

charges on any waters coordinated to the metal ion, and hence much greater acidity. The formation of what appears to be $[Cd(DPP)(OH)]^+$ as the pH is raised also means that the added stability provided by the coordinated hydroxides prevents EDTA from displacing DPP from Cd(II). This failure of EDTA to displace DPP was observed in attempted competition experiments between EDTA and DPP for coordination to Cd(II). Experiments of this type were used to determine log $K_1$ for PDA complexes.[35] One can discriminate between protonation equilibria that involve displacement of the metal ion, as in eq 4, and those that do not, as in eq 3 (formation of the MLOH complex). In its expression for log *K*, eq 4 contains no concentration of the metal ion, and consequently it was found that the protonation equilibrium for Gd(III), for example, that occurs at pH 5.17 was unaffected by changing the total Gd(III) concentration over 3 orders of magnitude ($2 \times 10^{-3}$, $2 \times 10^{-4}$, and $2 \times 10^{-5}$ M $Gd^{3+}$, with constant $4 \times 10^{-6}$ M DPP). On the other hand, the protonation equilibrium corresponding to eq 4 moved three pH units as the concentration of the metal ion was varied by 3 orders of magnitude, confirming our expectation that the equilibrium studied did involve the concentration of the metal ion.

Examination of the formation constants obtained for DPP in Table 5 shows some remarkable stabilities for the DPP complexes, as well as some remarkable metal ion selectivities. What immediately strikes one is the very high affinity of DPP for Cd(II), with selectivity (difference in log $K_1$ values) over Zn(II) of 4 log units. The high log $K_1$ value of 12.2 for Cd(II) means that at neutral pH the Cd(II) will be complexed below the $10^{-9}$ M level, considering the stabilizing effect of the $[ML(OH)]^+$ hydroxy complex. The smallest metal ion in Table 5, Ni(II), shows a remarkably low stability for its DPP complex, which seems reasonable in light of the arguments about chelate ring size and metal ion selectivity presented above. Unfortunately, no log $K_1$ values for quaterpy complexes, which would be the logical less-preorganized analogue of DPP, have been reported. The effect of the more rigid phen fragment of DPP as compared with the less preorganized quaterpy would be of considerable interest. The best that can be done now is to

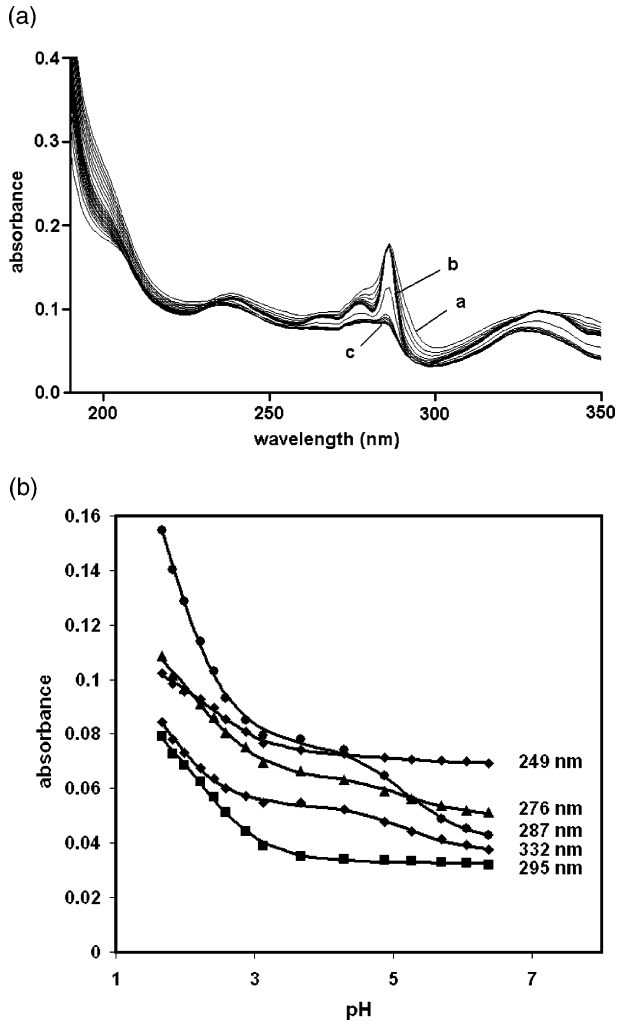


***Figure 6.*** (a) Electronic spectra of solutions of $4.0 \times 10^{-6}$ M DPP plus $10^{-3}$ M Gd(III) in 0.1 M $NaClO_4$ in the pH range 1.89−6.25. The spectrum at "a" is that at pH 1.89, where the complex is partly broken down to protonated forms of DPP. The spectra progress to "b" (pH 3.67) with rising pH, which is the point where the Gd/DPP complex is completely formed. With further rise in pH to "c" (pH 4.29 and above) it appears that a water molecule coordinated to the Gd(III) is being deprotonated, as discussed in the text. (b) Variation of absorbance of $4 \times 10^{-6}$ M DPP (= L) plus $2 \times 10^{-4}$ M $Gd(ClO_4)_3$ solution in 0.1 M $NaClO_4$ as a function of pH at five different wavelengths. The solid lines are theoretical curves fitted using SOLVER[47] with apparent protonation constants of 5.17 and 2.52, plus molar absorbtivities for the $LH_2^{2+}$, ML, and MLOH species at each wavelength. A value of $R^2$ of 0.9990 for the fit was obtained.

compare log $K_1$ for the DPP, phen, bipy, and the terpy complexes, as seen in Table 7. Table 7 shows that for small metal ions, such as Zn(II) and Ni(II), DPP forms complexes of very low stability when compared with log $\beta_2$ for bipy. The $[M(bipy)_2]^{n+}$ complexes make a reasonable comparison with the mono-DPP complexes, since they both have a four-nitrogen donor set. Metal ions that may be somewhat too small (Mn(II), In(III)) or somewhat too large (Pb(II), La(III), Ca(II)) for the cleft of DPP show moderate stabilization of log $K_1$ for their DPP complexes compared to log $\beta_2$ for the bipy complexes. Apart from Bi(III), the Cd(II) ion is the only ion that shows a very large stabilization of its DPP complex compared to log $\beta_2$ for its bipy complex. The same pattern can be discerned in comparing log $K_1$ for the phen or terpy complexes with log $K_1$ for DPP. Table 7 shows that the more preorganized backbone of phen compared to bipy leads[37] to a fairly constant stabilization

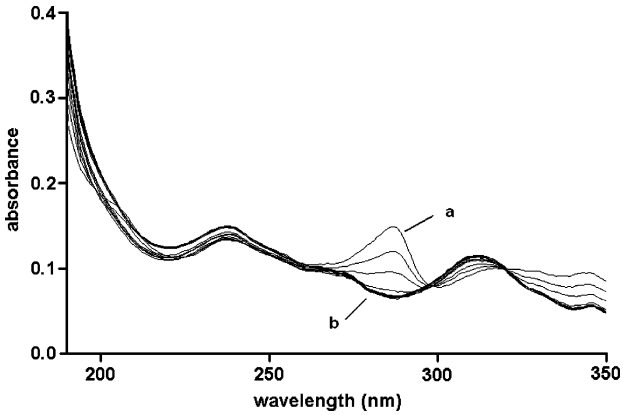


***Figure 7.*** Electronic spectra of solutions of $4.0 \times 10^{-6}$ M DPP plus $4 \times 10^{-6}$ M $Zn(ClO_4)_2$ in 0.1 M $NaClO_4$ in the pH range 1.89 to 6.25. The spectrum at "a" is that at pH 1.86, where the complex is broken down to protonated forms of DPP. The spectra progress to "b" (pH 6.17), where the Zn/DPP complex is completely formed.

of about 1.5 log units. By extrapolation from log $K_1$ for bipy (4.2) through terpy (6.1) for Cd(II), one might expect log $K_1$ for the Cd(II) quaterpy complex to be about 8.0. If this is correct, then the DPP complex of Cd(II) would be stabilized relative to the quaterpy complex by some 4.2 log units. This stabilization is considerably greater than the 1.5 log units observed for reinforcing bipy to give phen. The greater stabilization of the DPP complex may be due to difficulty in solvating the donor atoms in the cleft of DPP. This difficulty in solvating donor atoms resembles that proposed[49] for nitrogen-donor macrocyles, where it is proposed that steric hindrance to solvation of the donor atoms in the cavity of the macrocycle leads to enhanced thermodynamic stability for the metal−ligand complexes.

**Structural Studies.** The structures of **1**−**3** are shown in Figures 2−4, and bond lengths and angles of interest are given in Tables 2−4. The stereochemistry of coordination of pyridine-based ligands is of considerable interest, not only for ligands such as DPP or other polypyridyl ligands in Figure 1, but for pyridyl ligands in general, where these have been used to generate supramolecular structures with extended polypyridines complexing multiple metal ions,[50,51] or in the use of 4,4′-bipyridyl to synthesize metal trimers or tetramers with designed central cavities.[52,53]

A dominant factor in pyridyl-containing ligands is[37] the steric crowding produced by the *o*-hydrogen atoms on pyridines. Pyridine is a sterically crowding ligand, and a search of the CSD reveals very few $[M(py)_6]^{n+}$ complexes. There is a Ru(II) complex,[54] where one assumes that the strong Ru−N bonds compensate for the steric strain in the $[Ru(py)_6]^{2+}$ complex. Other examples involve large metal ions such as Yb(III)[55] ($r^+$ = 0.87 Å), Na(I) ($r^+$ = 1.02),[56] or Hg(II)[57] ($r^+$ = 1.02 Å), for

(49) Cabbiness, D. K.; Margerum, D. W. *J. Am. Chem. Soc.* **1969**, *91*, 6540.
(50) Constable, E. C.; Hougen, I. A.; Housecroft, C. E.; Neuberger, M.; Schaffner, S.; Whall, L. A. *Inorg. Chem. Commun.* **2004**, *7*, 1128.
(51) Constable, E. C.; Elder, S. M.; Healy, J.; Ward, M. D.; Tocher, D. A. *J. Am. Chem. Soc.* **1990**, *112*, 4590.
(52) Stang, P. J.; Cao, D. H.; Saito, S.; Arif, A. M. *J. Am. Chem. Soc.* **1995**, *117*, 6273.
(53) Kryschenko, Y. K.; Seidel, S. R.; Arif, A. M.; Stang, P. J. *J. Am. Chem. Soc.* **2003**, *125*, 5193.
(54) Templeton, J. L. *J. Am. Chem. Soc.* **1979**, *101*, 4906.
(55) Piecnik, C. E.; Liu, S.; Liu, J.; Chen, X.; Meyers, E. A.; Shore, S. G. *Inorg. Chem.* **2002**, *41*. 4936.
(56) Xie, X.; McCarley, R. E. *Inorg. Chem.* **1996**, *35*, 2713.
(57) Akesson, R.; Sandstrom, M.; Stalhandske, C.; Persson, I. *Acta Chem. Scand.* **1991**, *165*, 45.

***Table 6.*** Comparison of p$K_a$ Values of DPP Complexes with Those of the Corresponding Metal Aqua Ions[a]

| metal ion (M) | Cd(II) | Gd(III) | Lu(III) | Pb(II) | In(III) |
|---|---|---|---|---|---|
| $pK(M^{n+} = M(OH)^{(n-1)+} + H^+)$ | 10.1 | 7.7 | 7.3 | 7.6 | 3.9 |
| $pK(M(DPP)^{n+} = M(DPP)(OH)^{(n-1)+} + H^+)$ | 6.0 | 5.1 | 5.5 | 5.7 | 3.24 |

[a] Data from ref 40 (metal aqua ions, ionic strength = 0) and this work (DPP complexes). Waters left off the aqua ions and complexes for simplicity.

***Table 7.*** Comparison of Formation Constants for DPP with Those for Bipy, 1,10-phen, and Terpy[a]

| | | log *K* | | | | |
|---|---|---|---|---|---|---|
| | | bipy | | 1,10-phen | terpy | DPP |
| metal ion | $r^+$ (Å) | log $K_1$ | log $\beta_2$ | log $K_1$ | log $K_1$ | log $K_1$ |
| Ca(II) | 1.00 | 0.11 | 1.0 | 2.0[c] | 2.9 | |
| La(III) | 1.03 | 1.3 | ~2[b] | ~2 | 1.8[c] | 5.1 |
| Gd(III) | 0.94 | ~1.5[b] | ~2.4[b] | 2.2[c] | 6.2 | |
| Mn(II) | 0.80 | 2.6 | ~ 5.1[b] | 4.0 | 4.4 | 6.4 |
| Ni(II) | 0.67 | 7.0 | 13.9 | 8.7 | 10.7 | 6.8 |
| Zn(II) | 0.74 | 5.1 | 9.6 | 6.4 | 9.8[c] | 8.7 |
| Cd(II) | 0.96 | 4.2 | 7.8 | 5.7 | 6.1[c] | 12.2 |
| Pb(II) | 1.19 | 3.1 | ~5.1[b] | 4.6 | 6.0[c] | 7.8 |
| In(III) | 0.80 | 4.8 | 8.0 | 6.3 | 8.3 | |
| Bi(III) | 1.03 | 4.2 | ~7.0[b] | (14.8) | | |

[a] Data for bipy, 1,10-phen, and terpy from ref 40. [b] Estimated by comparison with the phen or other bipy or terpy complexes. [c] Unpublished work, Anhorn, M. J.; Hancock, R. D. *Ionic radii for octahedral coordination*, ref 38.

example. When a fairly small metal ion such as Mg(II) ($r^+$ = 0.74 Å) forms[58] an $[M(py)_6]^{2+}$ complex, the M−N bonds are rather long, with Mg−N averaging 2.28 Å. There is no crystallographic evidence that small metal ions such as Ni(II) ($r^+$ = 0.67 Å) or Co(III) ($r^+$ = 0.55 Å) can form $[M(py)_6]^{n+}$ complexes. Simple MM calculations[59] where M−N length is varied[60] suggest that for metal ions with M−N much less than 2.4 Å, steric strain due to nonbonded repulsions between *o*-hydrogens in $[M(py)_6]^{n+}$ complexes becomes severe. When pyridyl groups are connected together to form polypyridyls, many of the *o*-hydrogens are removed in forming the C−C bonds to hold the pyridyl groups together, and steric crowding is greatly reduced. In ligands such as bipy, terpy, or quaterpy, there is still the problem of H−H nonbonded repulsions between H3 and H3′ in the *syn*-conformation required for metal complexation. As the free ligand, these systems adopt an *anti*-conformation, which relieves the problem of H−H repulsion. In phen, the central fused benzo ring completely eliminates this problem.

The structure of $[Cd(DPP)_2]^{2+}$ (**1**) (Figure 3) shows an 8-coordinate Cd(II) with Cd−N(1) of 2.559 Å, and Cd−N(2) of 2.412 Å. Only five structures of 8-coordinate Cd(II) are found in the CSD,[44] that have bipy or phen ligands coordinated to the Cd(II). The Cd−N bonds in these average 2.41 ± 0.06 Å, in line with the idea that Cd−N(2) is a normal Cd−N bond, and that DPP coordinates to Cd(II) in a low strain fashion. The N(2)-Cd−N(2) angle in **1** is 68.19°, again in line with the N−Cd−N angles in 8-coordinate Cd(II) complexes of bipy and phen, which average 69.2 ± 2.4°. The Cd−N(1) bonds to the outer pyridyl groups of DPP are rather long, and not in accord with the expectation that DPP would form a complex with Cd(II) of the ideal geometry expected from the very high thermodynamic stability of the Cd(II) complex. The long Cd−N(1) bonds can

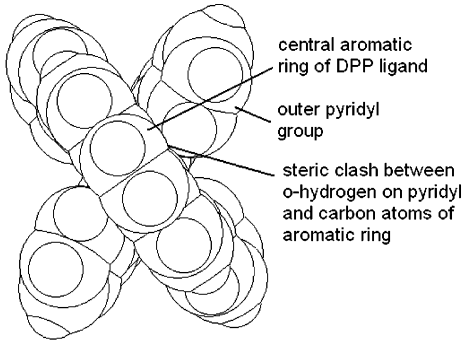


***Figure 8.*** Space-filling drawing of $[Cd(DPP)_2]^{2+}$ cation from **1**, showing the steric clashes between the *o*-hydrogens on the outer pyridyl groups of one DPP and the central aromatic ring of the other DPP ligand. To relieve the steric strain, the DPP ligands twist and become nonplanar so as to increase the H−C nonbonded distances. Drawing made with HyperChem.[59]

be understood using molecular mechanics (MM) calculations.[59] The stretching of the Cd−N(1) bonds in **1** is related to the twisted form of the DPP ligands in **1**, shown in Figure 8. The structure of $[Cd(DPP)_2]^{2+}$ is quite well reproduced using the extended version of the MM2 MM force field[61] present in HyperChem.[59] Starting with planar DPP ligands in $[Cd(DPP)_2]^{2+}$, the MM generates the twist present in the structure of **1** (Figure 8) which can be traced to nonbonded repulsions between the o-hydrogen atoms on one DPP ligand, and the carbons of the central aromatic ring of the other DPP ligand. The C−H nonbonded distances between these atoms are 2.86 Å, as compared to the sum of the van der Waals radii[62] of H and C of 2.90 Å. This small amount of compression suggests that the DPP ligand in **1** was quite easily twisted to alleviate the C−H nonbonded repulsions. MM calculations suggest that in $[Cd(DPP)(H_2O)_2]^{2+}$, the DPP ring would be planar in the absence of the C−H repulsions present in the bis-DPP complex, and the Cd−N bonds would have normal lengths in accord with the idea that DPP in the mono-complex with Cd(II) coordinates in a sterically efficient manner.

The structure of the $[Pb(DPP)(H_2O)(ClO_4)_2]$ complex (**2**) is seen in Figure 3a and b, showing the two different structures present in the unit cell. In both structures, the Pb is 8-coordinate, including long bonds (2.913−3.222 Å) to the perchlorate oxygens. The Pb−N bond lengths are 2.49−2.56 Å to the phen nitrogens, and 2.62−2.66 Å to the outer pyridyls. There is a coordinated water with Pb−O of 2.38 and 2.48 Å in the two structures. The Pb−$OH_2$ and Pb−N lengths, are relatively short for Pb-L bonds. These short bonds, together with the long Pb−O perchlorate bonds, suggest[63−67] that the Pb(II) is *hemidirected*,[66]

(58) Giannini, L.; Solari, E.; Zanotti-Gerosa, A.; Floriani, C.; Chiesa-Villa, A.; Rizzoli, C. *Angew. Chem., Int. Ed. Engl.* **1996**, *35*, 2825.
(59) *Hyperchem program*, version 7.5; Hypercube, Inc.: Waterloo, Ontario.
(60) Hancock, R. D. *J. Inclusion Phenom. Mol. Recognit. Chem.* **1994**, *17*, 63.
(61) Allinger, N. L. *J. Am. Chem. Soc.* **1977**, *98*, 8127.
(62) Bondi, A. *J. Phys. Chem.* **1964**, *68*, 441.
(63) Hancock, R. D.; Shaikjee, M. S.; Dobson, S. M.; Boeyens, J. C. A. *Inorg. Chim. Acta* **1988**, *154*, 229.
(64) Shimoni-Livny, L.; Glusker, J. P.; Bock, C. P. *Inorg. Chem.* **1998**, *37*, 1853.
(65) Reger, D. L.; Collins, J. E.; Rheingold, A. L.; Liable-Sands, L. M.; Yap, G. P. A. *Inorg. Chem.* **1997**, *36*, 345.
(66) Shimoni-Livny, L.; Glusker, J. P.; Bock, C. P. *Inorg. Chem.* **1998**, *37*, 1853.

i.e., that the lone pair on the Pb(II) is stereochemically active. One should point out here that DFT studies[68] suggest that the idea of the lone pair is not accurate, and that this "lone pair" of electrons distorts the geometry around Pb(II) by occupying antibonding orbitals. However, the concept of the lone pair is useful to our discussion. The stereochemically active lone pair results[63] in (1) an apparent gap in the coordination geometry or very long Pb−L bonds at the proposed site of the lone pair, (2) very short bonds on the side of the Pb(II) opposite the proposed site of the lone pair, and (3) the Pb−L bonds become progressively shorter as one moves around the Pb(II) from the site of the lone pair to the site opposite the lone pair. There are three oxygen donors from perchlorates bound to each Pb, with Pb(1)−O distances of 2.913, 2.972, and 3.222 Å, and Pb(2)−O distances of 2.642, 3.041, and 3.130 Å. One perchlorate to Pb-(1) is chelating, whereas Pb(2) forms bridges with one of the two perchlorates to which it is bound. These rather long Pb−O bonds are on the sides of the two Pb atoms away from the short Pb−O bonds to the water molecule, and the two short Pb−N bonds to the central nitrogens of the DPP ligands, suggesting that the lone pair in each case is located in the area on the Pb-(II) that produces the long Pb−O bonds to the perchlorates. The shorter Pb−N bonds to the central nitrogens (N(2) and N(3)) of the DPP ligand in Figure 3a are thus probably related to the geometry of the Pb(II) when it is hemidirected,[66] namely that the shortest Pb−L bonds are found on the side of the Pb(II) away from the lone pair. The DPP ligands in the Pb(II) complex are not quite planar, which probably relates to the variation in Pb−N bond length caused by the location of the lone pair more or less opposite the two central N-donors of the DPP ligand.

The structure of $[Hg(DPP)(ClO_4)_2]$ (**3**) is seen in Figure 4. The Hg is 8-coordinate, including the four M−N bonds to DPP, two Hg−O bonds to a chelating $ClO_4^-$, and two Hg−O bonds to two perchlorates that bridge between two Hg atoms, as shown in Figure 4. From a search of the CSD,[44] eight appears to be the maximum coordination number for Hg(II). There are only 35 8-coordinate structures out of a total of 3135 structures reported containing Hg(II).[44] The four M−N bonds in **3** are quite short compared to those in the Cd(II) and Pb(II) DPP structures. An eight-coordinate Hg(II) structure with two phen ligands[69] has Hg−N averaging 2.34 Å. The Hg−N bonds to the outer pyridyl groups in **3** are 2.250−2.258 Å, with an N−Hg−N bond angle of 155.21°. This is typical of structures of Hg(II), where the tendency toward linear two-coordination is discernible[67] in complexes with much higher coordination numbers. One thus frequently observes two short bonds at approximately 180° to each other in such structures, with the remaining Hg−L bonds being rather long, and at roughly right angles to the two short bonds. An example of this tendency is seen[70] in an Hg(II) complex with a crown ether, where the short axial Hg−Cl bonds to two chlorides are 2.34 Å, while bonds to the crown ether oxygens at roughly right angles to the Hg−Cl bonds average 2.88 Å. The DPP ligand in **3** is twisted rather like that in **1**, and one concludes from the structures reported here that the DPP ligand is quite easily twisted into a nonplanar conformation when coordinated to a metal ion.

**Fluorescence Studies.** Cadmium is the metal of interest in this study as far as fluorescence is concerned. In Figure 9a a 3-D fluorescence plot[45] for $10^{-8}$ M DPP ligand alone is seen. There is weak fluorescence with peaks at about 325 and 525 nm, with an exciting radiation of 300 nm. In the presence of an excess of $Cd^{2+}$, there is a strong emission at 385 nm with the same exciting radiation. In Figure 9b, this peak for $10^{-8}$ M DPP has an intensity of 14.9 qse (quinine sulfate equivalents) in the presence of $10^{-7}$ M $Cd^{2+}$, which figure remains the same at larger excesses of $Cd^{2+}$. In $10^{-9}$ M $Cd^{2+}$, the intensity of this peak is still 4.9 qse, whereas in $10^{-10}$ M $Cd^{2+}$ it has fallen to 1.4 qse. The free ligand DPP at $10^{-8}$ M has a fluorescence intensity at 385 nm of 0.98 qse. These results suggest that a ligand such as DPP could reliably be used to detect $Cd^{2+}$ by the CHEF effect down to a concentration of $10^{-9}$ M. It was found that in the presence of $10^{-6}$ M $Zn^{2+}$, $Hg^{2+}$, and $Pb^{2+}$, the fluorescence of $10^{-8}$ M DPP was not significantly affected. The lack of a CHEF effect for Pb(II) and Hg(II) is normal,[17,18] but Zn(II) usually produces the best CHEF effects with a wide variety of ligands. The lack of a CHEF effect for Zn(II) with DPP here parallels the lack of a CHEF effect for Zn(II) with ligands of the L2 and L3 type[72,73] in Figure 1. In the latter cases the lack of a CHEF effect has been traced to the rigidity of the phen moiety of L2 and L3. The rigidity leads to very long Zn−N bonds, as seen in the crystal structures,[72,73] involving the saturated N-donors of the macrocyclic ring adjacent to the phen moiety, which limited overlap allows the lone pairs to still quench the fluorescence of the aromatic system. Other metal ions of interest as potential sources of interference in the CHEF sensing of $Cd^{2+}$ are the similarly sized[38] $Ca^{2+}$ and $Na^+$. The CHEF effect derives from tying up the lone pairs on donor groups such as the N-donors of DPP by formation of M−L bonds,[17,18] but is also due to rigidification on complex-formation of the aromatic system, which system is the source of the fluorescence. Thus, one might expect metal ions of suitable size, such as $Ca^{2+}$ and $Na^+$ to have at least a modest CHEF effect. As shown in Figure 9c and d, these ions are capable of producing a CHEF effect, but at much higher concentrations than $Cd^{2+}$, because of the much lower thermodynamic stability of their complexes. $Ca^{2+}$ produces a strong CHEF effect with DPP down to a concentration of $10^{-3}$ M, in agreement with the measured log $K_1$ of 2.9 in Table 5. The $Na^+$ ion produces a significant CHEF effect with DPP only when present in 1.0 M concentration, suggesting that log $K_1$ for $Na^+$ with DPP might be about 0. There is an interest in detecting $Cd^{2+}$ in both fresh water and seawater, and in seawater, the concentration of $Ca^{2+}$ at $10^{-3}$ M is high enough to interfere with detection of $Cd^{2+}$ by DPP. With DPP itself, the interference from $Ca^{2+}$ in seawater could probably be eliminated using masking ligands such as nitrilotriacetic acid (NTA), which with log $K_1 = 6.7$[40] with $Ca^{2+}$ could inhibit its complexing with DPP. However, NTA, like EDTA, would be too weakly complexing with $Cd^{2+}$ to inhibit its complexation with DPP. Seawater contains $Na^+$ of 0.1 M, so that $Na^+$ would probably not interfere in the sensing of $Cd^{2+}$

(67) Hancock, R. D.; Reibenspies, J. H.; Maumela, H. *Inorg. Chem.* **2004**, *43*, 2981.
(68) Walsh, A.; Watson, G. W. *J. Solid State Chem.* **2005**, *178*, 1422.
(69) Grdenic, D.; Kamenar, B.; Hergold-Brundic, A. *Cryst. Struct. Commun.* **1978**, *7*, 245.
(70) Holdt, H-J.; Muller, H.; Keilling, A.; Drexler, H.-J.; Muller, T.; Schwarze, T.; Schilde, U.; Starke, I. *Z. Anorg. Allg. Chem.* **2006**, *632*, 114.
(71) Bazzicalupi, C.; Bencini, A.; Bianchi, A.; Giorgi, C.; Fusi, V.; Valtancoli, B.; Bernado, M. A.; Pina, F. *Inorg. Chem.* **1999**, *38*, 3806.
(72) Bazzicalupi, C.; Bencini, A.; Berni, E.; Bianchi, A.; Fornasari, P.; Giorgi, C.; Valtancoli, B. *Eur J. Inorg. Chem.* **2003**, 1974.
(73) Charles, S.; Yunus, S.; Dubois, F.; Vander Donckt, E. *Anal. Chim. Acta* **2001**, *440*, 37.

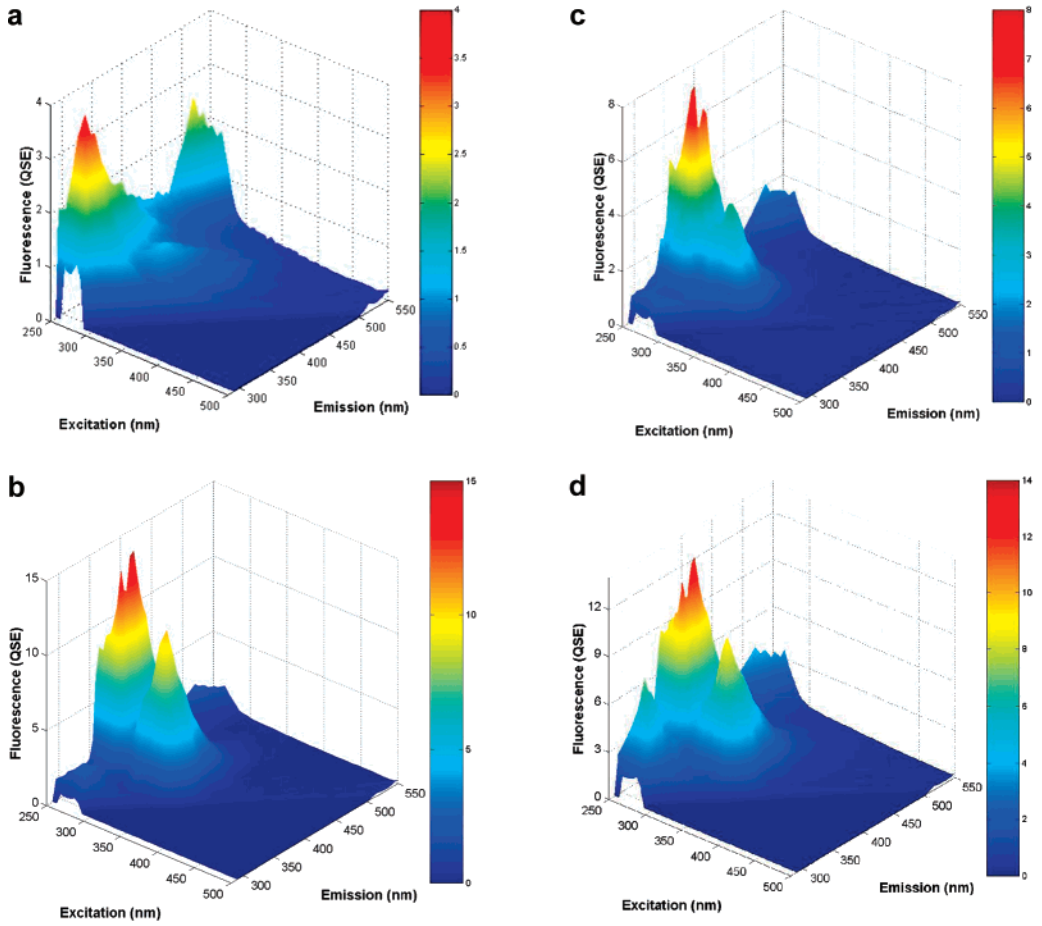


***Figure 9.*** (a) 3-D plot of fluorescence of the free DPP ligand ($10^{-8}$ M) at pH 7.0. The left-hand horizontal axis is the wavelength of the exciting radiation, whereas the right-hand horizontal axis is the wavelength of emission. The fluorescence intensity (vertical axis) is measured in QSE (quinine sulfate equivalents). Drawing made with the FLToolbox program.[45] (b) 3-D plot of fluorescence of the DPP ligand ($10^{-8}$ M) plus $10^{-7}$ M $Cd^{2+}$ at pH 7.0. The left-hand horizontal axis is the wavelength of the exciting radiation, whereas the right-hand horizontal axis is the wavelength of emission. The fluorescence intensity (vertical axis) is measured in QSE (quinine sulfate equivalents). Drawing made with the FLToolbox program.[45] (c) 3-D plot of fluorescence of the DPP ligand ($10^{-8}$ M) plus $10^{-2}$ M $Ca(ClO_4)_2$ at pH 7.0. The left-hand horizontal axis is the wavelength of the exciting radiation, whereas the right-hand horizontal axis is the wavelength of emission. The fluorescence intensity (vertical axis) is measured in QSE (quinine sulfate equivalents). Drawing made with the FLToolbox program.[45] (d) 3-D plot of fluorescence of the DPP ligand ($10^{-8}$ M) plus 1.0 M $NaClO_4$ at pH 7.0. The left-hand horizontal axis is the wavelength of the exciting radiation, whereas the right-hand horizontal axis is the wavelength of emission. The fluorescence intensity (vertical axis) is measured in QSE (quinine sulfate equivalents). Drawing made with the FLToolbox program.[45]

in seawater by CHEF. A previous method[73] of detecting $Cd^{2+}$ with L1 appears to have a detection limit without a preconcentration step of the $Cd^{2+}$ of about $10^{-7}$ M, so that the probable limit of detection of DPP with $Cd^{2+}$ of $10^{-9}$ M appears to be somewhat of an improvement. A fluorescent sensor for $Cd^{2+}$ based on terpy[74] has a detection limit of only $10^{-6}$ M $Cd^{2+}$, as is also one based[75] on di(2-picolyl)amine. In the latter case, the reported[75] stronger fluorescence of $Cd^{2+}$ than $Zn^{2+}$ is difficult to understand because di-2-picolylamine complexes more strongly with $Zn^{2+}$ than $Cd^{2+}$, and there is nothing in the architecture of the ligand that would lead to poor coordination of the $Zn^{2+}$, and hence weak fluorescence, as found here with DPP, or by other workers.[72,73]

It appears that $Cd^{2+}$ concentrations as low as $10^{-7}$ M in seawater may present a problem in that shellfish are able to accumulate Cd at these low concentrations.[76] Unpolluted oceanic waters have $Cd^{2+}$ concentrations[76] of about $10^{-10}$ M. Ideally, one would like to detect such low concentrations. DPP forms complexes of sufficient stability that it should complex $Cd^{2+}$ at these levels, but the fluorescence ability would have to be enhanced somewhat by, for example, replacing the pyridyl groups on DPP with other groups with more extended aromatic systems such as quinolyl groups, or construction of a larger aromatic system by addition of groups to the phen part of DPP. A reviewer has pointed out that the traditional approach for detecting low levels of $Cd^{2+}$ in the environment has been anodic stripping voltammetry,[77] with a detection limit of 1 ng/kg, or approximately $10^{-12}$ M. It would seem that with a log $K_1$ for DPP with $Cd^{2+}$ of 12.2 reported here, that with suitably enhanced fluorescent groups, a ligand of the DPP type should be able to match this performance.

## Conclusions

DPP demonstrates a high level of preorganization for a nonmacrocyclic ligand as well as remarkable thermodynamic stability in its complexes with metal ions having an ionic radius

(74) Luo, H.-Y.; Jiang, J.-H.; Zhang, X.-B.; Li, C.-Y.; Shen, G.-L.; Yu, R.-Q. *Talanta* **2007**, *72*, 575.
(75) Peng, X.; Du, J.; Fan, J.; Wang, J.; Wu, Y.; Zhao, J.; Sun, S.; Xu, T. *J Am. Chem. Soc*. **2007**, *129*, 1500.
(76) Kerfoot, W. B.; Jacobs, S. A. *Environ. Sci. Technol*. **1976**, *10*, 662.
(77) Mart, L.; Nuernberg, H. W.; Valenta, P.; Fresenius, S. Anal. Chem. **1980**, *300*, 350.

of about 1.0 Å. The rigidity of the five-membered chelate rings formed by DPP accounts for its selectivity for larger over smaller metal ions such as Ni(II) and Zn(II). The extended aromatic system of DPP provides an excellent combination of coordinating groups and fluorophores. DPP is a member of a largely unrecognized class of ligands, including the previously reported[35] PDA, that achieve levels of preorganization rivaling, or even exceeding, those of macrocyclic ligands, but which derive their high levels of preorganization from the rigidity provided by extended aromatic systems and not a cyclic structure.

**Acknowledgment.** GZ and RPT thank the Robert A. Welch foundation and the Division of Chemical Sciences, Office of Basic Energy Sciences, U.S. Department of Energy (Contract No. DE-FG03-02ER15334) for financial support. RDH and GMC thank the University of North Carolina Wilmington for generous financial support.

**Supporting Information Available:** Crystallographic information. This material is available free of charge via the Internet at http://pubs.acs.org.

JA077141M